Synthesis and Electrocatalytic Activity of the Delafossite-type Oxide Powders for the Methane Oxidation in a Solid Oxide Fuel Cell

(デラフォサイト型酸化物粒子合成と固体酸化物燃料電池におけるメタン酸化に対する電極触媒活性)

環境材料科学研究室 99585688　Teera Pinyowattayakorn
指導教官　佐藤　一則

1. Introduction

Carbon dioxide is the one of the greenhouse gases that are most significantly contributing to climate change. In Japan, about 304 million tons of equivalent carbon converted from the CO_2 –exhausted amount were released into the atmosphere in 1998[1]. The concentration of carbon dioxide in the earth's atmosphere can be affected by using energy more efficiently. Fuel cell is one of the renewable energy resources that can utilize hydrogen from any hydrocarbon fuel ; natural gas, ethanol, methanol. The high energy conversion efficiency can be expected to 40% - 60% with fuel cell because it converts the chemical energy of a fuel into electrical energy directly without combustion. While the efficiency for diesel engine is 25-35% and 20-25% for gasoline engine, 15-25 % for gas turbine engine [2].

The basic elements of a fuel cell consist of an electrolyte phase in intimate contact with a porous anode (negative electrode) and a porous cathode (positive electrode). Fuel (e.g. H_2 or methane gas) is fed to the anode where it is oxidized and electrons are released to the external circuit. Oxidant (e.g. oxygen) is fed to the cathode where it is reduced and electrons are accepted from the external circuit . The electron flow (from the anode to the cathode) through the external circuit produces direct-current electricity. The electrolyte conducts ions between two electrodes. Solid electrolyte structure in the SolidOxide Fuel Cell (SOFC) helps eliminate the material corrosion and electrolyte management problems. Figure 1 shows the SOFC structure.

Each component serves several functions in the fuel cell and must meet certain requirements such as the proper stability, in oxidizing and/or reducing environments, chemical compatibility with other components, and proper conductivity. SOFCs have potential ability to directly use hydrocarbon fuels, primarily methane. When using hydrocarbon gases such as CH_4 as a fuel, the internal reforming of CH_4 to H_2 and the direct oxidation of CH_4 gas will occur at the anode. To promote the reforming reaction and the direct oxidation, the materials that have high catalytic activity for the electrochemical oxidation of fuel such CH_4 would be desirable.

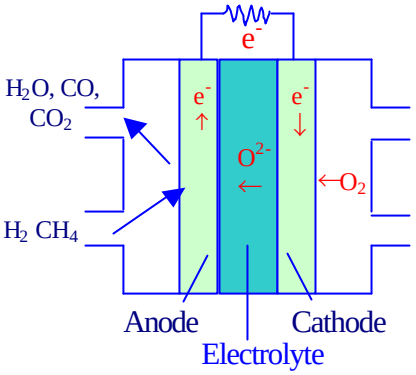

Fig. 1 SOFC single cell structure

For this research, the delafossite-type oxides including noble metals was applied as the catalyst to promote the direct anodic oxidation of CH_4 at low temperatures (about 850℃ or lower) in an SOFC system. The delafossite-type oxide powder has an ABO_2 structure in which A is noble metal element such as Pd, Pt, Ag and Cu , B is one of the transition elements such as Co, Fe, Cr. $PdCoO_2$ shows very low resistivities in the μΩ.cm order perpendicular to the c-axis at room temperature[3-5]. $PdCoO_2$

and $PtCoO_2$ are metallic conductors since the A-site ions in these compositions have an insufficient number of d electrons to fill the metallic bands completely. Pd shows an unusual monovalent state in a two fold, linear site, coordinated with two oxygen atoms, and oxygen is in a distorted tetrahedral-site, coordinated with three Co and one Pd atoms. In addition, $PdCoO_2$ was recently found that it shows the high catalytic activity for the anodic oxidation of methane gas (CH_4) [6]. However, from the past researches, the particle synthesis method in which the crystallization and particle size effect to the fuel cell performance still have size variation.

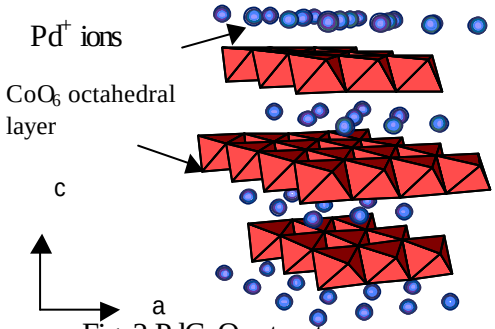

Fig. 2 $PdCoO_2$ structure

This research was aimed to synthesize uniform, well crystallined and fine $PdCoO_2$ particles. The increasing electrocatalytic activity caused by the addition of $PdCoO_2$ particles into a porous anode matrix was evaluated. Additionally, the synthesis of another delafossite structure-$PtCoO_2$ which has almost same electrical conductivity with $PdCoO_2$ was performed.

2. Experimental method

2.1 Synthesis of $PdCoO_2$ and $PtCoO_2$ particles by the co-precipitation method

$PdCoO_2$ and $PtCoO_2$ particles were synthesized by the Co-precipitation method. $PdCl_2$ (Palladium (II) Chloride) and $CoCl_2.6H_2O$ (Cobalt (II) Chloride Hexahydrate) are main raw starting materials for $PdCoO_2$. $PtCl_2$ (Platinum (II) Chloride) and $CoCl_2.6H_2O$ (Cobalt (II) Chloride Hexahydrate) are main starting materials for $PtCoO_2$ particle synthesis. Both $PdCoO_2$ and $PtCoO_2$ particles were synthesized in the Pt tubes that were encapsulated in quartz tubes and calcined in normal atmosphere at 750 ℃ for 1 hour as shown in Fig.3.

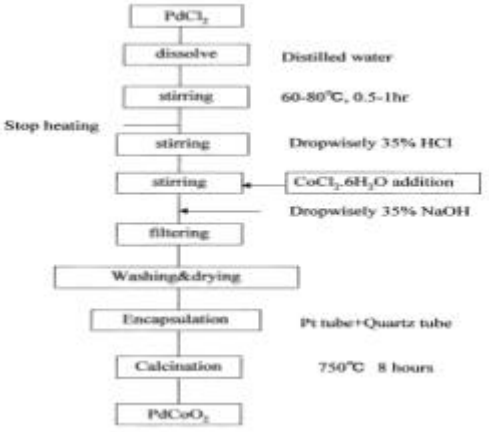

Fig. 3 $PdCoO_2$ synthesis by the co-precipitation method

2.2 Cell performance measurement

The ytteria stabilized-zirconia , ZR-8Y(8mol%Y_2O_3) disc (Nikato) was used as an oxygen ion conducting solid electrolyte. Pt paste (Tanaka Kikinzoku) was used as the cathode, followed by calcining in air at 1200℃ for 1 hour. As the anode, 2 wt% $PdCoO_2$ was mixed with Pt paste and smeared on one surface of the electrolyte disc as thinly possible by a pick, followed by calcining in air at 850℃ for 1 hour. The Pt meshes and Pt wires were attached to both sides of cell as output terminal. The cell was fabricated as shown Fig.4.

As fuel, methane and hydrogen gas mixed with helium gas was fed to the anode. Oxygen as oxidant gas was fed to the cathode.

A multi-channel digital multimeter (Keithley , model 2700) combined with its data acquisition system (Xlinx software) were used and the data were recorded in a personal computer via a GP-IB interface. The furnace was operated between 600℃-900℃.

For the measurement of the polarization properties of $PdCoO_2$ added-anode, the current

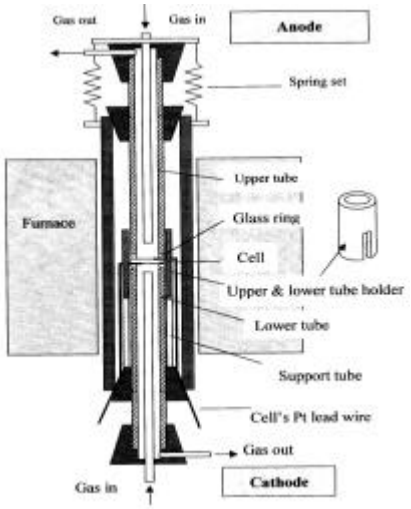

Fig.4 Cell assembly structure

interruption was used. The measurement circuit is shown in Fig. 5. The pulse generator or function generator and Potentiostat / Galvanostat as a current supply were used to generate 1ms pulse range of fixed current value (varying from 1, 3, 5, 7, 10, 15, 20, 40, 60, 80, 100 mA) to the electrolyte through the working electrode (WE) to the reference eletrode (RE). Comparing to the reference electrode, the potential change of WE to RE was measured with a digital oscilloscope.

The cell fabrication procedure for anodic polarization measurement was same as those for cell performance measurement.

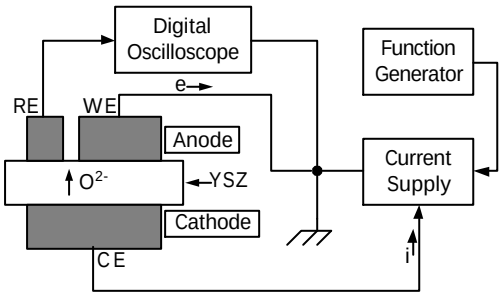

Fig.5 Anodic polarization measurement circuit diagram

3. Results and Discussion

3.1 $PdCoO_2$ and $PtCoO_2$ particles synthesis

Figure 6 shows the SEM image of the $PdCoO_2$.

$PdO.xH_2O$ or $Pd(OH)_2$ and $Co(OH)_2$ were precipitated in the chloride solution by adding a certain amount of NaOH solution. Subsequent calcinations for these precipitates at 750℃ for 8 hours resulted in a formation of fine $PdCoO_2$ particles(JCPDS# 27-1324) as shown in equation (1) with only a slight amount of PdO, Co_3O_4, and Pd. The synthesized $PdCoO_2$ particles showed a very high degree of crystal orientation perpendicular to the c-axis. The grain size of $PdCoO_2$ particles was in the range 10-20 μm. The formation of $PdCoO_2$ particles was examined by XRD data as shown in Fig. 7.

$$Pd(OH)_2 + Co(OH)_2 \rightarrow PdCoO_2 + 2H_2O \quad (1)$$

$$PtCl_2 + Co(OH)_2 + \frac{1}{2}O_2 \rightarrow PtCoO_2 + H_2O + Cl_2 \quad (2)$$

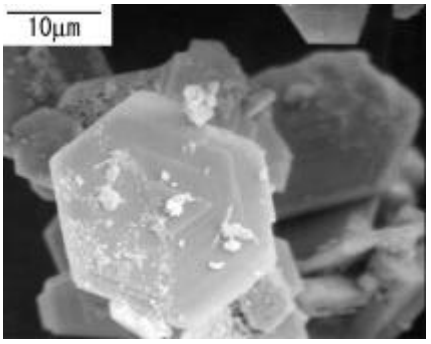

Fig. 6 $PdCoO_2$ particles

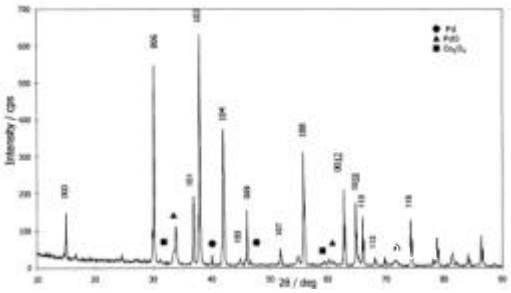

Fig. 7 XRD patterns of $PdCoO_2$ particles

Figure 8 shows the SEM image of the $PtCoO_2$ particles synthesized by the co-precipitation method. $PtCoO_2$ was first time successfully synthesized from the chloride

compound solutions of $PtCl_2$ and $CoCl_2.6H_2O$ in a closed system at 750℃ for 8 hours. The grain size of $PtCoO_2$ particles was smaller than 2 μm.

Figure 9 shows the XRD pattern for the $PtCoO_2$ particles (JCPDS file# 27-1330). For the $PtCoO_2$ particles synthesized in a sealed Pt tube, the sharp and high-intensity $PtCoO_2$ reflections were identified. However, small amounts of Pt and Co_3O_4 were detected as the weak reflection peaks. The X-ray diffraction pattern of the precipitates show only $PtCl_2$ and $Co(OH)_2$. The diffraction pattern can be identified to the $PtCoO_2$ phase. According to the above result, the $PtCoO_2$ phase can be formed as shown in the equation (2).

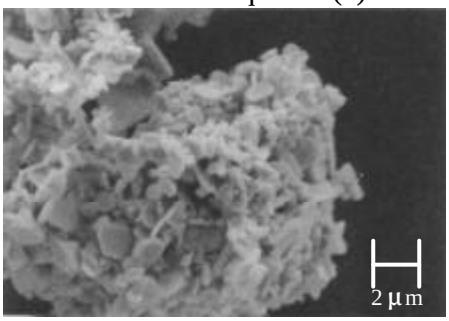

Fig. 8 $PtCoO_2$ particles

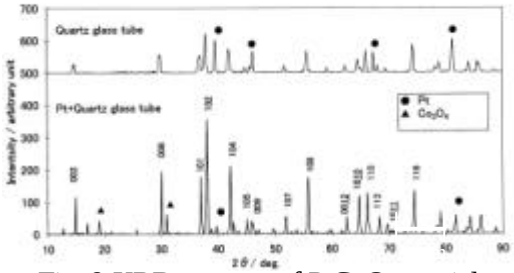

Fig. 9 XRD patterns of $PtCoO_2$ particles

SEM images of these particles showed small hexagonal plates with fine size about 2μm or less. These well crystallized particles could be expected to exhibit high electrocatalytic activity. Further study on the electrocatalytic activity of the $PtCoO_2$ dispersed anode should be made.

3.2 Electrocatalytic activity of the $PdCoO_2$ particles for methane oxidation

Figure 10 shows the temperature dependence of the maximum power densities for the cell using the $PdCoO_2$ -dispersed anode. The maximum power densities indicate that the fuel cell performance was higher for H_2 than for CH_4 .

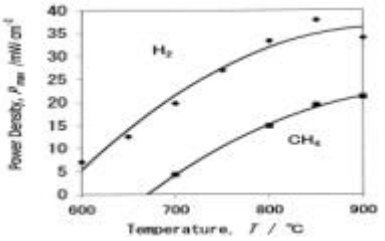

Fig. 10 Temp. dependence of maximum power density

Figure 11 shows that the dispersion of the $PdCoO_2$ particles into the anode enhanced the performance only when CH_4 was used as the fuel, the maximum power density at 850℃ increased about 3 times compared with the anode without any additive.

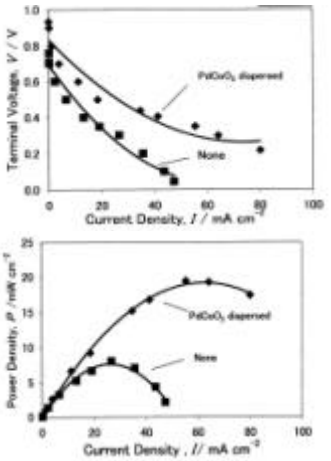

Fig. 11 Cell performance comparison between $PdCoO_2$-dispersed and non-dispersed cells

For the anodic polarization measurement, the current interruption method was applied. The IR drop due to the electrolyte resistance and overpotential generated at the interface between

electrolyte and the electrode can be separated from each other.

The Arrhenius plots of the inverse anodic polarization (R_p^{-1}) for each fuel gas were shown in Fig. 12. The $PdCoO_2$-dispersed anode cell clearly exhibited lower anodic polarization values than those for non-dispersed cell and ($PdO+Co_3O_4$)- dispersed cell at all temperature ranges.

$$CH_4 + O^{2-} \rightarrow CO + H_2 + 2e^- \qquad (3)$$

$$CH_4 \rightarrow C + 2H_2 \qquad (4)$$

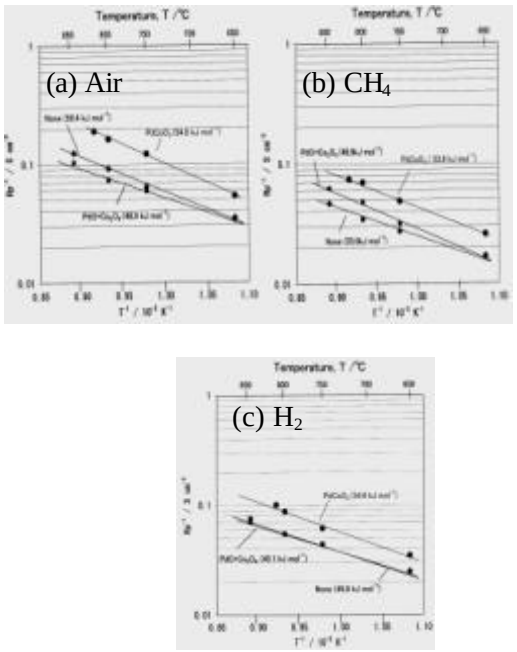

Fig. 12 Arrhenius plots of the inversed polarization resistance on various fuel gases

According to eqs. (3) and (4) , the enhancement of the CH_4 conversion to CO and H_2 by $PdCoO_2$ at the same discharge current well explains about the behavior of the Arrhenius plots for the inverse polarization resistance as shown in Fig. 12. For any fuel gas, $PdCoO_2$-dispersed anode has the highest R_P^{-1} value or compared with the non-dispersed anode and $PdO+Co_3O_4$-dispersed anode. This can be explained by the relation of the exchange current density (I_0) and R_P in the equation (5). Additionally, the dispersion of well and fine crystallized $PdCoO_2$ particles into the anode would increase the reaction area.

$$I_0(a+b) = \frac{RT}{R_p F} \qquad (5)$$

For the non-dispersed anode, the activation energy increased considerably upon changing from H_2 to CH_4 but for $PdCoO_2$-dispersed anode, the activation energies are almost the same for CH_4. The inverse polarization (R_P^{-1}) difference between the $PdCoO_2$ dispersed anode and non-dispersed anode also exhibit the larger polarization drop for CH_4. These results might be described as the effect of $PdCoO_2$ dispersion into the anode causing the high CH_4 oxidation activation. This is probably due to the combustion and subsequent steam-reforming reaction of CH_4

$$CH_4 + H_2O \rightarrow 3H_2 + CO \qquad (6)$$

The Pd monovalent state with two-fold coordination by the oxygen ions is stabilized in combination with trivalent cobalt ions that are mostly covalently bonded to the surrounding oxygen ions. This feature in $PdCoO_2$ is most likely to produce favorable reaction sites for the anodic oxidation of methane in the triple-phase area of the gas, anode and electrolyte.

In conclusion, the porous electrode finely dispersed with $PdCoO_2$ particles shows a high catalytic activation for the anodic oxidation of methane for the SOFCs based on the zirconia electrolyte. The high electrocatalytic activity of $PdCoO_2$ is caused by the specific valence states of both the Pd and Co ions as well as high electrical conductivity along the two-dimensional Pd layer.

4. Conclusion

(1) By the co-precipitation method, precipitates of $Pd(OH)_2$ and $Co(OH)_2$ were obtained and subsequent formation of the well crystallined and fine $PdCoO_2$ particles was made by the calcinations for the precipitates.

(2) $PtCoO_2$ particles with the delafossite structure were successfully synthesized for the

first time by the co-precipitation method. The reaction between $PtCl_2$ and $Co(OH)_2$ precipitates results in a formation of fine $PtCoO_2$ particles. The grain size is less than 2μm in average size with very high crystallization.

(3) The dispersion of fine $PdCoO_2$ particles into the anode can increase cell performance. The $PdCoO_2$-dispersed cell shows the temperature dependence, the CH_4 concentration dependence, the reproducibility of cell.

(4) The anodic polarization resistance showed a high $PdCoO_2$ catalytic activity for the electrochemical indicating the activation of the steam reforming reaction occurring at the surface active sites of $PdCoO_2$.

5. References

(1) EDMC/**エネルギー・経済統計要覧、日本エネルギー経済研究所** (http://www.eccj.or.jp)

(2) **田川博章**, **固体酸化物燃料電池と地球環境**, **アグネ承風社**, p.25 (1998).

(3) M. Tanaka et. al., "Origin of the metallic conductivity in $PdCoO_2$ with delafossite structure", Physica B, vol. 245, 157-163(1998).

(4) R. D. Shannon, D. B. Rogers, C. T. Prewitt, "Chemistry of Noble Metal Oxides. I. Synthesis and Properties of ABO_2 Delafossite Compounds", Inorganic Chemistry, vol.10, no.4, 713-718 (1971).

(5) D. B. Rogers, R. D. Shannon, C. T. Prewitt, J. L. Gillson, "Chemistry of Noble Metal Oxides. III. Electrical Transport Properties and Crystal Chemistry of ABO_2 Compounds with the Delafossite Structure", Inorganic Chemistry, vol.10, no.4, 723-727 (1971).

(6) K. Sato, M. Takezawa, M. Kohno, and Y. Inoue : Prog. Battery & Battery Mater., vol.17, 137-143 (1998).